8. For a fault zone in the earth's crust, the two horizontal stresses may be unequal, but the assumption of equality does not change the order of magnitude of the results.
9. E. Charlaix, E. Guyon, E. Roux, *Transp. Porous Media* **2**, 31 (1987).
10. L. J. Pyrak-Nolte, N. G. W. Cook, D. D. Nolte, *Geophys. Res. Lett.* **5**, 1247 (1988).
11. This well-known formula is sufficient, provided the faulted rocks are much more deformable than the adjacent rocks, which is the case here because the faulted rocks presumably contain more cracks. The applicability of this formula to rock heating is discussed in L. N. Germanovich, A. P. Dmitriev, S. A. Goncharov, *Thermomechanics of Rock Fracture* (Gordon and Breach, London, in press).
12. I. N. Sneddon and M. Lowengrub, *Crack Problems in the Classical Theory of Elasticity* (Wiley, New York, 1969).
13. B. I. Shklovskii and A. L. Efros, *Electronic Properties of Doped Semiconductors* (Springer-Verlag, New York, 1984), chap. 5.
14. D. Stauffer, *Introduction to Percolation Theory* (Taylor and Francis, London, 1985).
15. As a result, we cannot apply a model of stress-induced anisotropy that is based on two sets of perpendicular cracks as in C. M. Sayers [*Transp. Porous Media* **5**, 287 (1990)].
16. I. Balberg, C. H. Anderson, S. Alexander, N. Wagner, *Phys. Rev. B* **30**, 3933 (1984).
17. L. Onsager, *Ann. N.Y. Acad. Sci.* **51**, 627 (1949).
18. I. Balberg, *Phys. Rev. B* **31**, 4053 (1985), and references therein.
19. ———, *Philos. Mag. B* **56**, 991 (1987).
20. $N\langle V_c\rangle$ means the average number of disk centers in the volume $\langle V_c\rangle$, but, if two disk centers are inside $\langle V_c\rangle$, it is not necessary that the disks will intersect each other. That NV_c is also equal to the average number of intersections per crack can be strictly proved for the case of 3-D percolation in disk-like cracks and for any other percolation object shape that can be described by a finite number of parameters. It is likely that the statement is true in any case.
21. P. C. Robinson, *J. Phys. A* **17**, 2823 (1984).
22. E. Charlaix, *ibid.* **19**, L533 (1986).
23. R. L. Salganik, *Mech. Solids* **8**, 135 (1973).
24. E. Charlaix, E. Guyon, N. Rivier, *Solid State Commun.* **50**, 999 (1984). This is a particular case of Eq. 7 because $\langle\sin\theta\rangle = \pi/4$ for $\beta_c = \pi/2$ (*16*).
25. K. Hadley, *J. Geophys. Res.* **81**, 3483 (1976).
26. P. Gente, J. M. Auzende, V. Renard, Y. Fouquet, D. Bideau, *Earth Planet. Sci. Lett.* **78**, 224 (1986).
27. Y. Fouquet, G. Auclair, P. Cambon, J. Etoubleau, *Mar. Geol.* **84**, 145 (1988).
28. R. K. Hose and B. E. Taylor *U.S. Geol. Surv. Open File Rep. 74-271* (1974).
29. We appreciate the many helpful comments by the reviewers of earlier versions of this manuscript. This work was supported by the National Science Foundation under grant OCE 9012665 to R.P.L. L.N.G. thanks Parsons Brinckerhoff-KBB, Inc., Houston, TX, for supporting this work while he was in their employ.

8 October 1991; accepted 15 January 1992

Voltage-Dependent Calcium Channels in Plant Vacuoles

OMAR PANTOJA, ANGIE GELLI, EDUARDO BLUMWALD*

Free calcium (Ca^{2+}) in the cytoplasm of plant cells is important for the regulation of many cellular processes and the transduction of stimuli. Control of cytoplasmic Ca^{2+} involves the activity of pumps, carriers, and possibly ion channels. The patch-clamp technique was used to study Ca^{2+} channels in the vacuole of sugar beet cells. Vacuolar currents showed inward rectification at negative potentials, with a single-channel conductance of 40 picosiemens and an open probability dependent on potential. Channels were inhibited by verapamil and lanthanum. These channels could participate in the regulation of cytoplasmic Ca^{2+} by sequestering Ca^{2+} inside the vacuole.

FLUCTUATIONS IN THE AMOUNT OF cytoplasmic calcium (Ca^{2+}_{cyt}) are involved in the regulation of many cellular processes in animal cells (*1*); thus the concentrations of Ca^{2+}_{cyt} must be under tight control. In most animal cells, increases in the amount of Ca^{2+}_{cyt} occur as Ca^{2+} moves through selective channels in the plasma membrane and in the membrane of intracellular organelles (mainly the endoplasmic reticulum) (*1*). Decreases in the amount of Ca^{2+}_{cyt} occur primarily through the activity of Ca^{2+} pumps and Na^+/Ca^{2+} exchangers (*2*).

Similarly, Ca^{2+}_{cyt} regulates the physiology of plant cells. Several cellular aspects are affected, including phototropism and geotropism (*3*), ion fluxes in the vacuole (tonoplast) and plasma membrane (*4*), and photosynthesis (*5*). It has been postulated that increases in Ca^{2+}_{cyt} in plant cells can be induced by inositol 1,4,5-trisphosphate ($InsP_3$)–stimulated Ca^{2+} channels found in the tonoplast (*6*). Decreases in the amount of Ca^{2+}_{cyt} may be controlled by plasma membrane–bound Ca^{2+} pumps (*7*) and tonoplast-bound H^+/Ca^{2+} antiports (*8*); the latter would sequester Ca^{2+} inside the vacuole. Here, we describe voltage-dependent channels that allow the movement of Ba^{2+} (used as a Ca^{2+} analog) into the vacuole of sugar beet cells.

Currents carried by Ba^{2+} (*9*) were recorded in the whole vacuole as well as in isolated outside-out patches of tonoplast (*10*). Vacuolar currents showed a strong inward rectification, that is, the magnitudes of the currents elicited by negative polarization of the vacuole were much larger than those elicited by positive polarization (Fig. 1A). Whole-vacuole inward currents reached steady state 2 to 3 s after the onset of the voltage pulse. When $BaCl_2$ was substituted by KCl on the cytoplasmic side of the vacuoles and the concentration of Ca^{2+}_{cyt} was less than 10^{-5} M (*11*), voltage pulses of between −100 and +100 mV elicited only small instantaneous currents (Fig. 1A, bottom). Thus, the inward rectification obtained with $BaCl_2$ is the result of Ba^{2+} moving into the vacuole and is not due to the movement of vacuolar Cl^- in the opposite direction. With vacuoles exposed to symmetrical $BaCl_2$ solutions, inward currents were not observed, suggesting that intravacuolar Ba^{2+} may have blocked these currents (*12*). Positive potentials elicited only small outward currents under both conditions (Fig. 1B). The magnitude of the inward currents, however, increased as the tonoplast potential was made more negative. The similarity of the results from both Ba^{2+} concentrations in Fig. 1B indicates that the currents may have reached saturation. The currents elicited in vacuoles exposed to the 100 mM KCl bathing solution were of smaller magnitude than those with Ba^{2+} and varied linearly in the range of voltage studied.

Calculations from the Boltzmann plot (Fig. 1C) indicate that the Ba^{2+} currents are less sensitive to the electric field across the vacuole than the Ca^{2+} currents in animal cells where the slope $z = 4$ (*13*). These results also suggest that the vacuolar Ba^{2+} currents require more energy to change from the closed to the open state, as compared to K^+ currents from the sarcoplasmic reticulum of muscle cells, where the Gibbs free energy $\Delta G_i = 1.56$ kcal mol^{-1} (*14*).

An estimate of the selectivity of the channels was obtained by the tail-currents method (Fig. 2). Inward currents reversed at 10 mV (E_{rev}) with 30 mM Ba^{2+} in the cytoplasmic side and 100 mM K^+ in the vacuole. Similar values were obtained from five different vacuoles. With this value of E_{rev} and using a modification of the Goldman-Hodgkin-Katz equation (*15*), we calculated a permeability ratio $P_{Ba^{2+}}/P_{K^+}$ of 2.3.

Currents inactivated within 10 min, thus preventing further characterization of the inward currents (Fig. 2C). The magnitude of the currents elicited by the activating voltage pulse to −100 mV decreased as the

Centre for Plant Biotechnology, Department of Botany, University of Toronto, Toronto, Ontario, Canada M5S 3B2.

*To whom correspondence should be addressed.

experiment proceeded, reaching about one-half the initial value within 5 min. This current decrease could not be accounted for by a partial resealing of the pipette, because at the end of every experiment the magnitude of the vacuolar capacitance remained unchanged (*12*).

Using outside-out patches, we resolved inward currents at the single-channel level (Fig. 3). The magnitude of the current moving through a single channel increased as the patch potential was made more negative. Clamping the patch of tonoplast to positive potentials failed to stimulate the opening of single channels. This result indicates that ion channels are the unitary entities for the macroscopic currents recorded in the whole-vacuole experiments. The open probability of the channels was dependent on the tonoplast potential, as shown by the increase in the number of channels opening simultaneously and also by an apparent increase in the mean open time (Fig. 3A). In contrast to the whole-vacuole currents, the single-channel currents did not inactivate with time and in some cases it was possible to record these currents over a period of 20 min. Single-channel currents of the tonoplast (I_{SC}) were blocked by specific inhibitors of Ca^{2+} channels in animal cells (Fig. 3B). In the presence of verapamil, only brief openings were observed with no apparent reduction in the magnitude of the I_{SC}, suggesting that this inhibitor may reduce the mean opening time, rather than plugging the channel, as observed for the inhibition of Ba^{2+} currents in ventricular cells by nitrendipine (*16*). Lanthanum (5 mM) inhibited the single-channel currents more strongly, as no openings were observed (*12*).

Single-channel current-voltage (I_{SC}-V) relations showed that the inward rectification—also observed in the whole vacuole—was a result of the inability of the channels to allow the movement of ions in the outward direction (Fig. 4A). The I_{SC}-V relations were approximately ohmic between 0 and −70 mV at any concentration of Ba^{2+}_{cyt}, with a slope conductance of about 40 pS for 100 mM Ba^{2+}_{cyt}, and the $P_{Ba^{2+}}/P_{K^+}$ ratio was 5 to 7. Between 10 and 100 mM Ba^{2+}_{cyt}, the extrapolated E_{rev} values moved toward the equilibrium potential for Ba^{2+} (Fig. 4A, arrows), further indicating that the inward rectifying currents were carried by Ba^{2+}. The magnitude of I_{SC} showed a tendency to saturate with increasing concentrations of Ba^{2+}_{cyt}, in accord with Michaelis-Menten kinetics (Fig. 4B). The saturation of the single-channel currents correlated well with the whole-vacuole experiments (see Fig. 1B).

Beet cell tonoplast has channels that allow the movement of Ba^{2+} into the vacuole in a voltage-dependent manner, showing a strong inward rectification at negative vacuolar potentials. The Ba^{2+} currents obtained in this work are through Ca^{2+}-selective channels. These tonoplast Ca^{2+} channels showed several properties comparable to those observed for L-type Ca^{2+} channels in animal cells (*15*): (i) the magnitude of I_{SC} saturates with increasing Ba^{2+}_{cyt}, with the dissociation constant K_d and the maximum current I_{max} close to those for animal cells (28 mM and 1.6 pA, respectively); (ii) there is a single-channel conductance with 100 mM Ba^{2+}_{cyt} of 40 pS as compared to that of 25 pS in ventricular myocytes; (iii) verapamil and La^{3+} inhibit the Ca^{2+} channel; (iv) there is a nonapparent inactivation of the single-channel currents; and (v) Sr^{2+} can substitute for Ba^{2+} as the

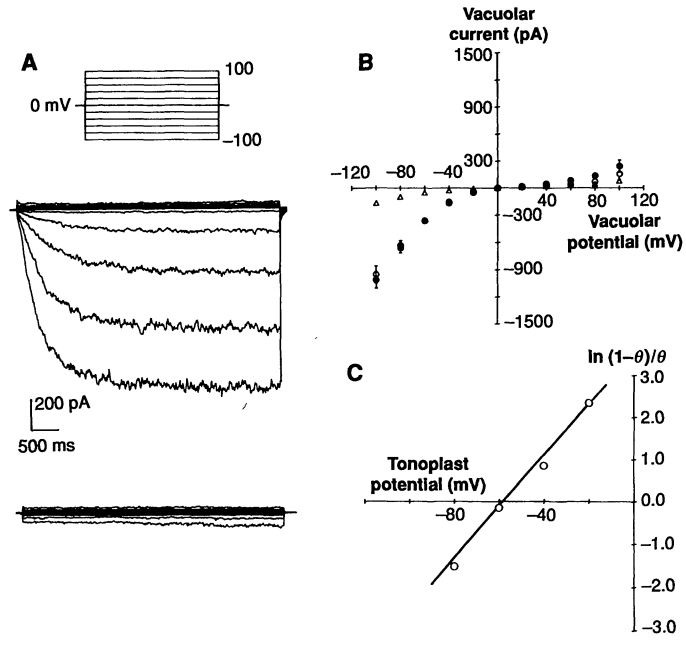

Fig. 1. Voltage-dependent Ba^{2+} currents in the whole-vacuole configuration. (**A**) (Top) Currents from intact vacuoles were elicited by the application of voltage pulses ranging from +100 to −100 mV from a holding potential of 0 mV. (Center) With vacuoles exposed to a bathing solution containing 30 mM $BaCl_2$, pulses up to +100 mV elicited only small instantaneous outward currents, whereas polarization of the vacuole to potentials more negative than −40 mV evoked large and time-dependent inward currents. (Bottom) Replacing $BaCl_2$ with 100 mM KCl in the bath solution eliminated the large time-dependent inward currents. (**B**) Current-voltage relations from whole-vacuole experiments. Inward currents recorded with 30 mM (●) or 50 mM (○) $BaCl_2$ in the bath were of similar magnitude at all negative potentials. With 100 mM KCl in the bath (△), the instantaneous currents showed a linear relation between +100 and −100 mV. (**C**) Boltzmann plot of the currents recorded with 30 mM $BaCl_2$ in the bath. The relative conductance (θ) is defined as the G/G_{max} ratio. The line is a least squares fit of slope (z) 1.6 and y-intercept of ΔG_i = 2.05 kcal mol^{-1}. Pipette solution (inside the vacuole) contained 100 mM KCl, 1 mM $CaCl_2$, 2 mM $MgCl_2$, 5 mM tris/MES, pH 5.5, adjusted to 450 mosmol with sorbitol. All bathing solutions contained 2 mM $MgCl_2$, 5 mM tris/MES, pH 7.5, and $BaCl_2$ or KCl at the concentrations indicated. Points are the mean ± SE of at least four measurements. Where the SE is not shown, it was smaller than the symbols.

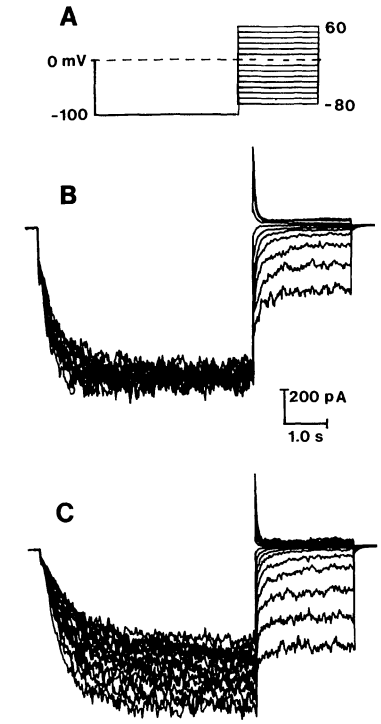

Fig. 2. Reversal potential and inactivation of the Ba^{2+} currents. (**A**) Inward currents were activated by −100-mV pulses for 5 s and deactivated from a steady level by stepping down the voltage to −80 mV. This protocol was repeated 15 times with the deactivation pulse increased by 10 mV for each following pulse. (**B**) The inward currents reversed direction at 10 mV. For clarity, only the responses to deactivating pulses between −60 and 30 mV are shown. (**C**) Inactivation of the Ba^{2+} currents during the recording of the reversal of the inward currents. The magnitude of the currents elicited by the activating voltage pulses decreased continuously from the first pulse (bottom trace) to the last one (upper trace). The duration of the experiment was 3.75 min. Bathing solution in both (B) and (C) contained 30 mM $BaCl_2$, and the pipette solution was as in Fig. 1.

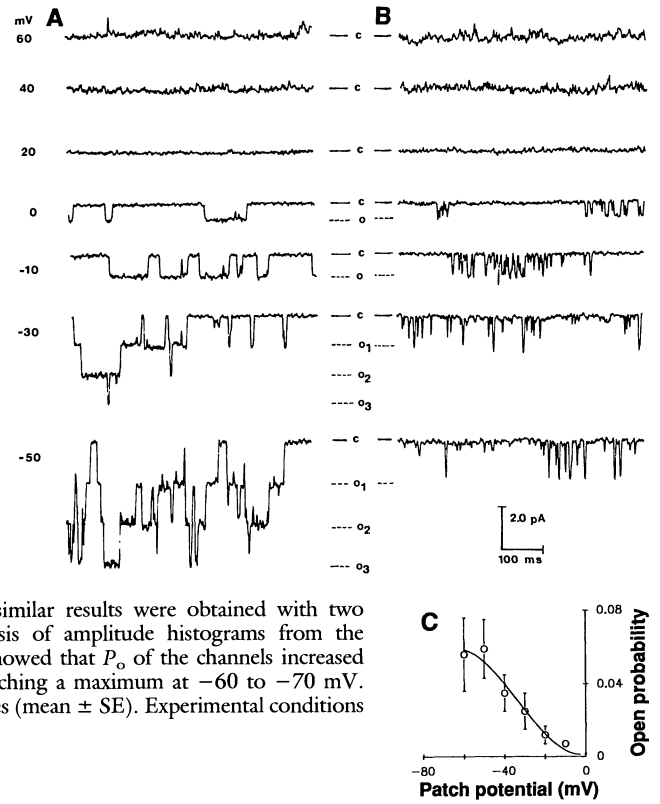

Fig. 3. Single-channel recordings of Ba^{2+} currents. Outside-out patches of tonoplast were continuously polarized to the voltages shown on the left. (**A**) Step-like events were recorded only when the patches of tonoplast were held at potentials of between 0 and −70 mV, indicating the opening (o) and closing (c) of single channels. The presence of more than one channel in the patches was indicated by the occurrence of simultaneous openings (o_1, o_2, . . ., o_n). (**B**) Addition of 250 μM verapamil to the bath inhibited the channel activity as indicated by the brief openings and the absence of simultaneous events. (A) and (B) are records from the same patch exposed to 50 mM $BaCl_2$; similar results were obtained with two different patches. (**C**) Analysis of amplitude histograms from the single-channel records (*20*) showed that P_o of the channels increased between 0 and −50 mV, reaching a maximum at −60 to −70 mV. Data from five different patches (mean ± SE). Experimental conditions were as in Fig. 2.

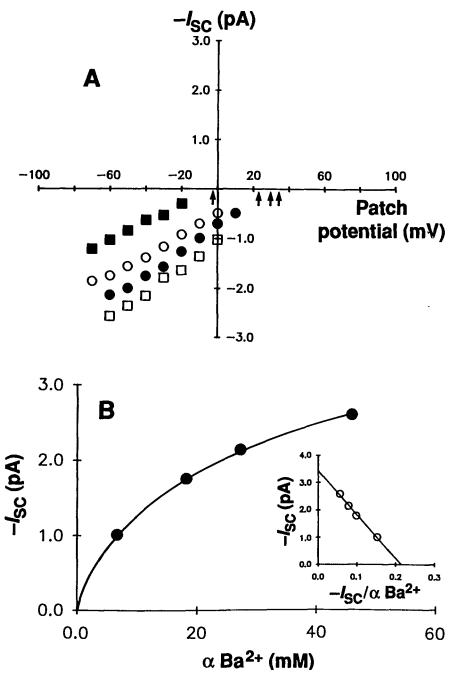

Fig. 4. (**A**) Current-voltage relations (I_{SC}-V) from single-channel recordings of tonoplast. With 100 mM KCl in the recording pipette and 10 mM (■), 30 mM (○), 50 mM (●), or 100 mM (□) $BaCl_2$ in the bath, the magnitude of the single-channel currents varied linearly with the patch potential. Least squares analysis gave E_{rev} of −3, 26, 29, and 33 mV (arrows) for 10, 30, 50, and 100 mM Ba^{2+}, respectively. (**B**) Dependence of I_{SC} amplitude on the activity (α) of $Ba^{2+}{}_{cyt}$. The I_{SC} values at −60 mV were plotted against α $Ba^{2+}{}_{cyt}$. The magnitude of I_{SC} showed an apparent saturation at 100 mM $Ba^{2+}{}_{cyt}$. The curve was fitted by eye. (Inset) Analysis of the experimental points with an Eadie-Hofstee plot gave an apparent K_d = 16.2 mM and a $I_{SC\ max}$ = −3.44 pA. Data are the mean ± SE of at least four patches.

charge carrier (*12*). However, several differences were observed: (i) the activation and inactivation kinetics in the vacuole of plant cells are much slower (seconds) than in animal cells (milliseconds) (*15*); (ii) the sensitivity of the currents to the electric field across the tonoplast is smaller (*13*); and (iii) the selectivity of the tonoplast channels between divalent and monovalent cations is much smaller than for the plasma membrane of animal cells (*15*).

Activation of the tonoplast inward rectifying Ca^{2+} channels may function as an alternative mechanism for the regulation of $Ca^{2+}{}_{cyt}$ in plant cells through a negative feedback mechanism. Under conditions that may induce the production of intracellular $InsP_3$ (that is, hormones or light) activation of outward Ca^{2+} channels in the tonoplast (*6*) would increase $Ca^{2+}{}_{cyt}$ levels with a concomitant polarization of the tonoplast to about −100 mV, close to the equilibrium potential for Ca^{2+} ($E_{Ca^{2+}}$) (*17*). Moreover, $Ca^{2+}{}_{cyt}$ would be further increased by the $InsP_3$-induced Ca^{2+} release from the endoplasmic reticulum (*18*). As a consequence, a higher cytoplasmic electrochemical potential for Ca^{2+} would be established, activating the vacuolar inward Ca^{2+} channels for the removal of $Ca^{2+}{}_{cyt}$. Regulation of the remaining $Ca^{2+}{}_{cyt}$ would be achieved by the plasma membrane Ca^{2+} adenosine triphosphatase (*7*) and the vacuolar H^+/Ca^{2+} antiport (*8*).

REFERENCES AND NOTES

1. J. R. Williamson and J. R. Monck, *Annu. Rev. Physiol.* **51**, 107 (1989); R. W. Tsien and R. Y. Tsien, *Annu. Rev. Cell Biol.* **6**, 715 (1990).
2. E. Carafoli, *Annu. Rev. Biochem.* **56**, 395 (1987).
3. C. A. Gehring, D. A. Williams, S. H. Cody, R. W. Parish, *Nature* **345**, 528 (1990).
4. R. Hedrich and E. Neher, *ibid.* **329**, 833 (1987); J. I. Schroeder and S. Hagiwara, *ibid.* **338**, 427 (1989).
5. M. Brauer, D. Sanders, M. Stitt, *Planta* **182**, 236 (1990).
6. J. Alexandre, J. P. Lassalles, R. T. Kado, *Nature* **343**, 567 (1990).
7. F. Rasi-Caldogno, M. C. Pugliarello, M. I. De Michelis, *Plant Physiol.* **83**, 994 (1987); S.-A. Briars, F. Kessler, D. Evans, *Planta* **176**, 283 (1988).
8. K. S. Schumaker and H. Sze, *Plant Physiol.* **79**, 1111 (1985).
9. We used Ba^{2+} as the main charge carrier for several reasons: (i) Ba^{2+} is much less effective than Ca^{2+} or Sr^{2+} at activating Ca^{2+}-dependent K^+ channels (*15*); therefore, activation of Ca^{2+}-dependent cation channels in the tonoplast of sugar beet (*4, 12*) was prevented; (ii) the magnitude of I_{SC} through Ca^{2+} channels is larger with Ba^{2+} than with Ca^{2+} (*15*); and (iii) Ba^{2+} blocks inward rectifying cation channels in the tonoplast of sugar beet [O. Pantoja, J. Dainty, E. Blumwald, *FEBS Lett.* **255**, 92 (1989)] that may interfere in the recording of Ca^{2+} currents.
10. The experimental procedure has been described in detail (*19*). Vacuoles were isolated by osmotic shock of protoplasts from sugar beet cells (*Beta vulgaris*). Patch-clamp techniques were used to record ionic currents from whole vacuoles and isolated outside-out patches [O. P. Hamill, A. Marty, E. Neher, B. Sakmann, F. J. Sigworth, *Pfluegers Arch.* **391**, 85 (1981)]. Pipettes with a tip resistance of 3 to 5 megohms were coated with silicone (Sigmacote, Sigma) and heat-polished. A vacuole-attached configuration with seals of 6 to 10 gigaohms was obtained. We minimized liquid junction potentials by filling the reference and recording pipettes with the same solution; both pipettes were connected to the patch-clamp amplifier (Dagan 3900, Minneapolis) and to ground through Ag-AgCl electrodes. Whole-vacuole recordings were obtained with the pCLAMP program (version 5.0, Axon Instruments) and data were stored in a PCII-386 computer operating on-line. The patch-clamp amplifier compensated for the series resistance and capacitative transients and measured the vacuolar capacitance. We recorded single-channel currents by continuously polarizing the isolated patches of tonoplast. The currents were digitized at 44 kHz by a pulse code modulator, stored on videotape (DAS 900, Dagan) and processed with the PAT V 6.1 program (J. Dempster, University of Strathclyde, Glasgow, U.K.). Whole-cell and single-channel recordings were low pass–filtered at 200 Hz with a four-pole Bessel filter contained in the patch-clamp amplifier. Experiments were performed at room temperature (20° to 23°C).
11. Free $Ca^{2+}{}_{cyt}$ was kept at levels ≈10^{-6} M (as measured with a Ca^{2+}-selective electrode (KWIKCAL, World Precision Instruments, Sarasota, FL) without the addition of Bapta, EGTA, or $CaCl_2$. The use of the chelators was avoided because of their similar affinities for Ca^{2+} and Ba^{2+} [(*12*); A. E. Martell and R. M. Smith, *Critical Stability Constants* (Plenum, London, 1974)].
12. O. Pantoja, A. Gelli, E. Blumwald, unpublished data.
13. B. Hille, *Ion Channels of Excitable Membranes* (Sinauer Associates, Sunderland, MA, 1984).
14. P. Labarca, R. Coronado, C. Miller, *J. Gen. Physiol.* **76**, 397 (1980).
15. R. W. Tsien, P. Hess, E. W. McCleskey, R. L. Rosenberg, *Annu. Rev. Biophys. Biophys. Chem.* **16**, 265 (1987); P. Hess, J. B. Lansman, R. W. Tsien, *J. Gen. Physiol.* **88**, 293 (1986):

$$E_{rev} = \frac{RT}{2F} \ln \frac{4\, P_D\, a_D\, [D]}{P_M\, a_M\, [M]} \quad (1)$$

where E_{rev} is the reversal potential; [D] and [M] are concentrations and P_D and P_M are the permeabilities of the divalent and monovalent ions, respectively; a_D and a_M are activity coefficients; R is the Boltzmann constant; T is temperature; and F is the Faraday constant.

16. P. Hess, J. B. Lansman, R. W. Tsien, *Nature* **311**, 538 (1984).
17. J. I. Schroeder and P. Thuleau, *Plant Cell* **3**, 555 (1991). With a vacuolar Ca^{2+} concentration of 10^{-3} M and with Ca^{2+}_{cyt} at 10^{-7} M, 10^{-6} M, and 10^{-5} M, values of $E_{Ca^{2+}}$ are −112, −84, and −56 mV, respectively.
18. M. J. Berridge and R. F. Irvine, *Nature* **341**, 197 (1989).
19. O. Pantoja, J. Dainty, E. Blumwald, *J. Membr. Biol.*, in press.
20. Open channel probabilities were calculated with amplitude histograms obtained from single-channel recordings as:

$$P_0 = \frac{\sum_{i=0}^{n} i \cdot A_i}{n \sum_{i=0}^{n} A_i} \quad (13)$$

where n is the number of channels in the patch, P_0 is the probability that any one channel is open, and A_i is the area under the peaks with i channels open (*14, 19*).

21. We thank J. Hellebust for reviewing the manuscript. This research was supported by an operating grant of the Natural Sciences and Engineering Research Council of Canada.

22 November 1991; accepted 27 January 1992

Structure, Expression, and Antisense Inhibition of the Systemin Precursor Gene

BARRY MCGURL, GREGORY PEARCE, MARTHA OROZCO-CARDENAS, CLARENCE A. RYAN*

A gene that encodes systemin, a mobile 18–amino acid polypeptide inducer of proteinase inhibitor synthesis in tomato and potato leaves, has been isolated from tomato, *Lycopersicon esculentum*. Induction of proteinase inhibitors in plants is a response to insect or pathogen attacks. The gene has 10 introns and 11 exons, ten of which are organized as five homologous pairs with an unrelated sequence in the eleventh, encoding systemin. Systemin is proteolytically processed from a 200–amino acid precursor protein, prosystemin. Prosystemin messenger RNA was found in all organs of the plant except the roots and was systemically wound-inducible in leaves. Tomato plants transformed with an antisense prosystemin complementary DNA exhibited greatly suppressed systemic wound induction of proteinase Inhibitor I and II synthesis in leaves.

PLANTS HAVE INDUCIBLE DEFENSES in response to pathogen or herbivore attacks (*1–4*), including systemic synthesis and accumulation of serine proteinase inhibitors that inhibit the digestive proteinases of insects and microorganisms (*5–8*). The wound-induced synthesis of such inhibitors results from transcriptional activation of the inhibitor genes (*9*) and has been described in a variety of species including tomato (*10, 11*), potato (*12*), alfalfa (*13, 14*), cucurbits (*15*), and poplar trees (*16*). Wounding results in the rapid accumulation of inhibitors not only in wounded leaves but also in distal, unwounded leaves, indicating that a signal, or signals, released from the wound site travels throughout the plant. Proposed signals include pectic fragments derived from the plant cell wall (*17*), the lipid-derived molecule jasmonic acid (*18*), the plant hormone abscisic acid (*19*), electrical potentials (*20, 21*), and an 18–amino acid polypeptide called systemin (*22*). Systemin was isolated from the leaves of tomato plants where it induces the synthesis of two proteinase inhibitors. Radioactively labeled systemin, when applied to a wound site, was rapidly translocated to distal tissues. We now report the cloning and characterization of the cDNA and gene encoding systemin.

We isolated a systemin cDNA by screening a primary cDNA library synthesized from tomato leaf mRNA with an oligonucleotide corresponding to amino acids 12 through 18 of systemin (*23*). Approximately 50 positive clones were identified and rescreened with a second oligonucleotide corresponding to amino acids 1 to 6 of systemin. Of the initial positive clones, only one hybridized to the second probe; it was a partial cDNA encoding the systemin polypeptide within a larger protein, prosystemin.

This partial cDNA consisted of 839 bp, although Northern (RNA) blot analysis indicated that the systemin mRNA was 1 kb. We determined the complete prosystemin mRNA sequence by sequencing the prosystemin gene (*24*) and mapping the transcriptional start site (*25*). The open reading frame was 600 bp encoding a 200–amino acid prosystemin protein (Fig. 1). Identification of the initiating methionine codon was made on the basis of two criteria: multiple stop codons immediately 5′ to the methionine codon and an adjacent sequence similar to the plant consensus sequence for translational initiation (*26*).

Of the 200–amino acid prosystemin, amino acids 179 through 196 encode systemin. Prosystemin contains a high percentage of charged amino acids (aspartic acid, 10%; glutamic acid, 17%; lysine, 15%) but very few hydrophobic amino acids and is therefore quite hydrophilic. We did not find a hydrophobic region at the NH_2-terminus that resembled a leader peptide, and the posttranslational processing pathway and site of subcellular compartmentalization of prosystemin are undetermined. Neither the cDNA nor the deduced protein precursor sequences had homologs in either GenBank or the European Molecular Biology Laboratory data bank.

The putative processing sites bordering systemin did not conform to the consensus sequence for endoproteolytic processing sites flanking bioactive peptides in animal prohormone precursors (*27*). The animal consensus sequence was, however, found once in prosystemin at amino acid residues 183 through 188, which are part of the mature systemin polypeptide. The half-life of systemin may be regulated by further processing at this site. In animal systems prohormones are often processed to yield multiple bioactive peptides (*28, 29*), although we have no evidence to suggest that other bioactive polypeptides are derived from prosystemin.

Prosystemin is encoded by a single gene that consists of 11 exons and 10 introns (Fig. 2, A and B). The transcriptional start

```
  1  MGTPSYDIKNKGDDMQEEPKVKLHH
 26  EKGGDEKEKIIEKETPSQDINNKDT
 51  ISSYVLRDDTQEIPKMEHEEGGYVK
 76  EKIVEKETISQYIIKIEGDDDAQEK
101  LKVEYEEEEYEKEKIVEKETPSQDI
126  NNKGDDAQEKPKVEHEEGDDKETPS
151  QDIIKMEGEGALEITKVVCEKIIVR
176  EDLAVQSKPPSKRDPPKMQTDNNKL
```

Fig. 1. Amino acid sequence of prosystemin (*38*). The systemin sequence is underscored with a double line. A polypeptide sequence element repeated five times is underscored with a single line. GenBank accession numbers for prosystemin cDNA and gene are M84800 and M84801, respectively.

Institute of Biological Chemistry, Washington State University, Pullman, WA 99164–6340.

*To whom correspondence should be addressed.